Published in final edited form as:
Brain Res. 2013 July 3; 1520: 145–156. doi:10.1016/j.brainres.2013.05.006.

Somatostatin receptor subtype-4 agonist NNC 26-9100 mitigates the effect of soluble $A\beta_{42}$ oligomers via a metalloproteinase-dependent mechanism

Karin E. Sandoval[1], **Susan A. Farr**[2,3], **William A. Banks**[4], **Albert M. Crider**[1], **John E. Morley**[3,5], and **Ken A. Witt**[1]

[1]Pharmaceutical Sciences, School of Pharmacy, Southern Illinois University Edwardsville, 200 University Park Drive, Edwardsville, Illinois

[2]Research and Development, Veterans Affairs Medical Center–St Louis, Missouri

[3]Department of Internal Medicine, Division of Geriatrics, Saint Louis University School of Medicine, Missouri

[4]Geriatric Research Education and Clinical Center-Veterans Affairs Puget Sound Health Care System, Seattle, Washington and Department of Internal Medicine, Division of Gerontology and Geriatric Medicine, University of Washington School of Medicine, Seattle, Washington

[5]Department of Internal Medicine, Division of Endocrinology, Saint Louis University School of Medicine, Missouri

Abstract

Soluble amyloid-β peptide (Aβ) oligomers have been hypothesized to be primary mediators of Alzheimer's disease progression. In this regard, reduction of soluble Aβ-oligomers levels within the brain may provide a viable means in which to treat the disease. Somatostatin receptor subtype-4 (SSTR4) agonists have been proposed to reduce Aβ levels in the brain via enhancement of enzymatic degradation. Herein we evaluated the effect of selective SSTR4 agonist NNC 26-9100 on the changes in learning and soluble $A\beta_{42}$ oligomer brain content with and without co administration of the M13-metalloproteinase family enzyme-inhibitor phosphoramidon, using the senescence-accelerated mouse prone-8 (SAMP8) model. NNC 26-9100 treatment (0.2 μg i.c.v. in 2 μL) improved learning, which was blocked by phosphoramidon (1 and 10 mM, respectively). NNC 26-9100 decreased total soluble $A\beta_{42}$, an effect which was blocked by phosphoramidon (10 mM). Extracellular, intracellular, and membrane fractions were then isolated from cortical tissue and assessed for soluble oligomer alterations. NNC 26-9100 decreased the $A\beta_{42}$ trimeric (12 kDa) form within the extracellular and intracellular fractions, and produced a band-split effect of the $A\beta_{42}$ hexameric (25 kDa) form within the extracellular fraction. These effects were also blocked by phosphoramdon (1 and 10 mM, respectively). Subsequent evaluation of NNC 26-9100 in APPswe Tg2576 transgenic mice showed a similar learning improvement and corresponding reduction in soluble $A\beta_{42}$ oligomers within extracellular, intracellular, and membrane fractions.

Corresponding Author: Ken A. Witt Ph.D., Department of Pharmaceutical Sciences, School of Pharmacy, Southern Illinois University Edwardsville, Campus Box 2000, Edwardsville, IL., 62026, Phone: 618-650-5144, Fax: 618-650-5145, kwitt@siue.edu.

No other disclosures.

These data support the hypothesis that NNC 26-9100 reduces soluble $A\beta_{42}$ oligomers and enhances learning through a phosphoramidon-sensitive metalloproteinase-dependent mechanism.

Keywords

Phosphoramidon, NNC 26-9100; Somatostatin receptor subtype-4; Amyloid beta oligomer

Introduction

Alzheimer's disease (AD) is a neurodegenerative condition characterized by a progressive loss in memory and cognitive abilities. The amyloid cascade hypothesis maintains that dysregulation of amyloid-β peptide (Aβ) within the brain initiates AD pathology (Serrano-Pozo et al., 2011). The steady-state levels of Aβ in the brain are maintained via the balance of production and clearance processes. Recent research implicates impaired clearance of Aβ from the brain as the principle factor in the non-familial late-onset form of AD (Mawuenyega et al., 2010), which accounts ~99% of AD cases (Alzheimer's Association, 2012). Clearance, in turn, is mediated by transport and enzymatic mechanisms. As such, even subtle changes in the transport or metabolic balance of Aβ over time could significantly influence the progression of AD. While alterations in Aβ transport mechanisms at the level of the blood-brain barrier (BBB) have been heavily investigated (Deane et al., 2009; Jeynes and Provias, 2011), any therapeutic application impacting the BBB is hindered by a number of factors (e.g. transporter adaptations, variable cerebrovascular health, potential impact on transport of other nutrients/waste-products). A more direct approach, albeit with limitations of its own, is to increase Aβ catabolism within the brain. In this regard, enzymatic degradation of Aβ as a means of treatment has received a significant deal of attention over the past decade. The catabolism of Aβ is controlled by several amyloid-degrading enzymes (ADEs). Of these ADEs, the M13 family of metalloproteinases appears to have the greatest potential to effectively mitigate Aβ levels within the brain (Nalivaeva et al., 2012; Saido and Leissring, 2012).

Among the functionally characterized members of the M13 family, neprilysin and neprilysin-2, as well as the neprilysin homologues: endothelial converting enzyme-1 and -2 (ECE1/ECE2), have shown substantial affinity for $A\beta_{40}$ and $A\beta_{42}$ (Nalivaeva et al., 2012; Saido and Leissring, 2012; Shirotani et al., 2001). Enhanced activity of these enzymes corresponds with significant decreases of Aβ within the brain in conjunction with increased cognitive function (Nalivaeva et al., 2012; Saido and Leissring, 2012). Moreover, neprilysin has shown to degrade soluble $A\beta_{42}$ oligomers (Huang et al., 2006; Iwata et al., 2005; Kanemitsu et al., 2003). There has been a significant amount of research focused on soluble $A\beta_{42}$ oligomers as potential mediators of AD pathology, as these soluble forms have shown to more closely correlate with dementia and synaptic loss than insoluble fibrillar deposits (Larson and Lesne, 2012; Lue et al., 1999; McLean et al., 1999; Mucke et al., 2000; Terry et al., 1991). Nevertheless, the principle caveat of direct manipulation of enzymatic processes for the treatment of AD is the significant potential for peripheral side effects. In this regard, selectively targeting upstream regulators of the M13 family within critical AD associated brain regions (i.e. cortex and hippocampus) is a more applicable approach in which to mitigate Aβ accumulation.

Somatostatin (somatotropin release-inhibiting factor; SRIF) is a cyclic peptide widely expressed throughout the central nervous system, shown to be involved in learning and memory processes (Epelbaum et al., 2009). Additionally, somatostatin has been identified as a principle regulator of neprilysin activity. Somatostatin administration has been shown to increase neprilysin activity, corresponding with decreased $A\beta_{42}$ levels, both *in vivo* and *in*

vitro (Saito et al., 2005). It has been hypothesized that the decreased somatostatin levels observed with AD progression are directly responsible for the loss of neprilysin activity and subsequent increases of $A\beta_{42}$ within the brain (Iwata et al., 2005; Saito et al., 2005). Such a cascade could also generate a positive feedback cycle, further lowering somatostatin levels and enzymatic activity, accelerating $A\beta_{42}$ accumulation and aggregation. Thus, agonists designed to act selectively upon somatostatin receptor (SSTR) subtypes within the brain could provide an effective means to enhance the action of neprilysin, and potentially other M13 enzymes associated with Aβ degradation, restraining such a pathological feedback loop.

The SSTRs can be divided into two families: SRIF-1 and -2. The SRIF-1 family is composed of subtypes 2, 3 and 5. The SRIF-2 family is composed of subtypes 1 and 4. Of the five subtypes, SSTR2 and SSTR4 have the highest brain expression (Kumar, 2005). While SSTR2 is highly expressed within the pituitary, controlling the release of neurohormones, SSTR4 has limited peripheral and pituitary distribution (Bruno et al., 1992; Moller et al., 2003). Moreover, SSTR4 is well expressed in cortical and hippocampal tissues (Bruno et al., 1992; Moller et al., 2003). In this regard, SSTR4 is the most practical target for a somatostatin-based therapeutic. We have recently evaluated the effects of both acute (i.c.v.) (Sandoval et al., 2012) and chronic (i.p.) (Sandoval et al., 2011) administration of the SSTR4 agonist NNC 26-9100 in the senescence accelerated mouse prone-8 (SAMP8) mouse model. The SAMP8 strain exhibits age associated learning and memory decline, corresponding with critical changes in brain tissue similar to those observed in late-onset AD (i.e. progressive elevation of oxidative processes, APP, Aβ, and hyperphosphorylated tau) without genetic modifications (Morley et al., 2012a; Morley et al., 2012b). Our previous results showed that NNC 26-9100 increased brain neprilysin activity, decreased levels of soluble $A\beta_{42}$ oligomers, and improved learning and memory (Sandoval et al., 2011; Sandoval et al., 2012). Nevertheless, the degree of interdependence of these effects remains to be determined.

Herein, we evaluated NNC 26-9100 enzyme dependent action on learning and soluble $A\beta_{42}$ oligomer alterations via co-administration of the M13 family enzyme inhibitor phosphoramidon in12-month old male SAMP8 mice. Following treatment and behavioral analysis, cortical tissues were extracted for evaluation of total soluble $A\beta_{42}$, and soluble $A\beta_{42}$ oligomers respective to cellular fractions (i.e. extracellular, membrane, and intracellular pools). Lastly, as much of the evidence of soluble Aβ oligomer toxicity has come from the use of transgenic mouse models, NNC 26-9100 impact was also assessed in APPswe Tg2576 mice for additional understanding and comparison.

1. Results

2.1 Phosphoramidon impact on NNC 26-9100 learning enhancement in SAMP8 mice

NNC 26-9100 is a stable non-peptide drug with high affinity and selectivity for SSTR4 (Ankersen et al., 1998; Crider et al., 2004). Dose of NNC 26-9100 (0.2 μg, i.c.v. in 2 μL) was based on previous work showing optimal learning effect (Sandoval et al., 2012). The 24 h post-injection time point was chosen for consistency with regards to testing paradigm, previous NNC 26-9100 data (Sandoval et al., 2012), and supporting evidence showing that somatostatin administration could increase neprilysin activity over 24 h corresponding to a decrease in $A\beta_{42}$ levels (Saito et al., 2005). The 12 month old male SAMP8 mice were used as they are a non-transgenic model that only exhibits soluble forms of Aβ at this age, with corresponding Aβ-dependent reductions cognitive function (Morley et al., 2000; Tomobe and Nomura, 2009). Dose range of phosphoramidon used was delineated from literature as to the effectiveness to impeded the M13 family associated catabolism of $A\beta_{42}$ (Eckman et al., 2001; Eckman et al., 2006; Saito et al., 2005; Shirotani et al., 2001).

NNC 26-9100 impact on learning was evaluated with and without co-administration of phosphoramidon (1 or 10 mM) in SAMP8 mice (n = 14-16/group) (Fig. 1). Mice treated with NNC 26-9100 showed a lower number of mean trials to first avoidance compared to vehicle ($P < 0.001$), demonstrating NNC 26-9100 improved acquisition learning. NNC 26-9100 treatment with either 1 mM phosphoramidon ($P < 0.001$) or 10 mM phosphoramidon ($P < 0.001$) increased the number of mean trials to first avoidance compared to NNC 26-9100 alone, demonstrating a blockade of NNC 26-9100 learning enhancement. No significant effect on the number of mean trials to first avoidance was shown between vehicle and vehicle + 1 mM phosphoramidon or vehicle + 10 mM phosphoramidon.

2.2 Phosphoramidon impact on total soluble $A\beta_{x\text{-}42}$ against NNC 26-9100 treatment in SAMP8 mice

NNC 26-9100 treatment effect on total soluble $A\beta_{42}$ within cortical tissue, with and without phosphoramidon (1 or 10 mM) co-administration, was measured via $A\beta_{x\text{-}42}$ enzyme-linked immunosorbent assay (ELISA) (n = 5-6/group) (Fig. 2). NNC 26-9100 treatment decreased $A\beta_{x\text{-}42}$ levels compared to vehicle alone ($P < 0.05$). NNC 26-9100 + 1 mM phosphoramidon treatment decreased $A\beta_{x\text{-}42}$ levels compared to vehicle + 1 mM phosphoramidon ($P < 0.01$). NNC 26-9100 + 10 mM phosphoramidon treatment showed identical levels of $A\beta_{x\text{-}42}$ compared to vehicles, and had increased $A\beta_{x\text{-}42}$ levels compared to the NNC 26-9100 alone ($P < 0.01$). No change between vehicle alone and vehicle + 1 mM phosphoramidon or vehicle + 10 mM phosphoramidon were observed.

2.3 Phosphoramidon impact on soluble $A\beta_{42}$ oligomers against NNC 26-9100 treatment in SAMP8 mice

Soluble $A\beta_{42}$ oligomer evaluations were conducted from extracellular, membrane, and intracellular enriched protein extractions of cortical tissues using Western blot (n = 4-5/group). Within the extracellular fraction, $A\beta_{42}$ oligomeric bands were shown at 56 (dodecamer; a.k.a. Aβ*56), 50, 40 (nonamer), 25 (hexamer), and 12 (trimer) kDa (Fig. 3). No discernible bands were identifiable below the 12 kDa, with exception of lane possessing the $A\beta_{42}$ positive control (4 kDa). This aspect is consistent with experimental conditions used for non-fibrillar soluble fractions (Lesne et al., 2006). No significant changes were found in the 56, 50, or 40 kDa bands across all groups. While NNC 26-9100 treatment did not significantly lower the 25 kDa band, the 25 kDa band displayed a split within the extracellular fraction. This split was negated when NNC 26-9100 was co administered with either 1 or 10 mM phosphoramidon. The extracellular 12 kDa trimer band showed a significant decrease with NNC 26-9100 treatment ($P < 0.01$), which was reversed by co-administration of both 1 and 10 mM phosphoramidon ($P < 0.05$).

Within the membrane fraction, $A\beta_{42}$ oligomers were observed at 56, 50, and 25 kDa (Fig. 4). No significant changes were shown within this fraction for any treatment group.

The $A\beta_{42}$ oligomers within the intracellular fraction were observed at 56, 50, 25, and 12 kDa (Fig. 5). While no changes were observed across treatments within the 56, 50, or 25 kDa bands, there was a decrease in the 12 kDa band with NNC 26-9100 treatment ($P < 0.01$). The decrease in the intracellular 12 kDa band was reversed by co-administration of 1 and 10 mM phosphoramidon ($P < 0.01$ and $P < 0.05$, respectively).

No significant changes were shown in any $A\beta_{42}$ oligomer form between vehicle alone and vehicle + 1 mM phosphoramidon or vehicle + 10 mM phosphoramidon, within any cellular fraction.

2.4 NNC 26-9100 learning impact in Tg2576 mice

While use of the SAMP8 model is appropriate for the evaluation phosphoramidon dependent activity, as addressed within the introduction, a group of APPswe Tg2576 mice was evaluated using the same NNC 26-9100 dose (0.2 μg, i.c.v. in 2 μL) against vehicle control. The treatment of the 12-month old male APPswe mice was identical in all manners to that of the SAMP8 mice. At 11-13 months of age APPswe mice show a 14-fold increase in $A\beta_{1-42}$ over those at 2-8 months of age, with appreciable deficits in learning and memory over younger mice (Hsiao et al., 1996). NNC 26-9100 impact on learning was assessed against vehicle control (n = 3-4) (Fig. 6A). NNC 26-9100 treatment showed a lower number of mean trials to first avoidance compared to vehicle ($P < 0.05$), demonstrating NNC 26-9100 improved acquisition learning in APPswe mice, consistent with that of age-matched SAMP8 mice.

2.5 NNC 26-9100 impact on $A\beta_{42}$ oligomers in Tg2576 mice

Soluble $A\beta_{42}$ oligomer levels from Tg2576 mice were conducted from extracellular, membrane, and intracellular enriched protein extractions of cortical tissues (n = 3-4/group). Within the extracellular fraction, $A\beta_{42}$ oligomeric bands were found at 56 (a.k.a. Aβ*56), 50, 40, 25, and 12 kDa (Fig. 6B & 6C). A decrease in the extracellular 56 ($P < 0.05$), 25 ($P < 0.01$), and 12 ($P < 0.001$) kDa bands with NNC 26-9100 treatment were observed. The 25 kDa band displayed a band-split within the extracellular fraction, similar to that observed in SAMP8 mice.

Within the membrane fraction, $A\beta_{42}$ oligomers were observed at 70, 56, 50, 40, and 25 kDa (Fig 6B & 6D). Only the 25 kDa band showed a decrease with NNC 26-9100 treatment ($P < 0.05$).

The $A\beta_{42}$ oligomers within the intracellular fraction were observed at 56, 50, 40, 25, and 12 kDa (Fig. 6B & 6E). There was a decrease with NNC 26-9100 treatment for the 25 ($P < 0.05$) and 12 ($P < 0.001$) kDa bands.

2.6 NNC 26-9100 impact on $A\beta_{40}$ oligomers in Tg2576 mice

Soluble $A\beta_{40}$ oligomer levels from Tg2576 mice were conducted from extracellular, membrane, and intracellular enriched protein extractions of cortical tissues (n = 3-4/group). Within the extracellular fraction, $A\beta_{40}$ oligomeric bands were found at 75, 63, 56, 40, 25, and 12 kDa (Fig. 7A & 7B). A decrease in the extracellular 75 ($P < 0.01$), 63 ($P < 0.01$), 40 ($P < 0.05$) and 12 ($P < 0.001$) kDa bands with NNC 26-9100 treatment was observed.

Within the membrane fraction, $A\beta_{40}$ oligomers were observed at 75, 56, 45, 40, 25 and 18 kDa (Fig 7A & 7C). The 45 and 40 kDa bands showed a decrease with NNC 26-9100 treatment ($P < 0.01$). No other significant changes were observed with treatment within this fraction.

The $A\beta_{40}$ oligomers within the intracellular fraction were observed at 75, 56, 45, 40, 25, and 12 kDa (Fig. 7A & 7D). No other significant changes were observed with treatment within this fraction.

3. Discussion

The M13 family of enzymes has been identified to be primary mediators of Aβ catabolism within the brain. As such, these enzymes have significant pathological and therapeutic implications towards AD. Selective enhancement of SSTR4 action within the brain has the potential to mitigate toxic $A\beta_{42}$ oligomer accumulation via regulation of these enzymes.

Herein, we investigated the impact of the selective and high affinity SSTR4 agonist NNC 26-9100 with regards to enzymatic dependent action on soluble $A\beta_{42}$ oligomers.

The effects of NNC 26-9100 on learning were measured using the T-maze foot shock avoidance test, against the enzyme inhibitor phosphoramidon. We used an optimized dose of NNC 26-9100 previously shown to improve learning and increase cortical neprilysin activity in 12-month old SAMP8 mice (Sandoval et al., 2012). The time-frame also corresponds with work showing somatostatin administration was capable of increasing neprilysin activity (Iwata et al., 2005; Saito et al., 2005). Critically, co-administration of phosphoramidon reversed the learning improvement shown with NNC 26-9100 treatment at both 1 and 10 mM. These data support the hypothesis that NNC 26-9100 impacts learning via an metalloproteinase-dependent mechanism.

Subsequent to behavioral analyses, cortical tissues were processed for examination of both total and cellular fraction content of soluble $A\beta_{42}$. ELISA evaluation showed a decrease in total soluble $A\beta_{x\text{-}42}$ with NNC 26-9100 treatment, paralleling the work by Saito and colleagues showing a similar effect with somatostatin (Saito et al., 2005). While the NNC 26-9100 treatment effect on $A\beta_{x\text{-}42}$ was inhibited with co-administration of 10 mM phosphoramidon, it was not inhibited by 1 mM phosphoramidon. This disparity may simply be a concentration dependent effect, as phosphoramidon does differentially inhibit the M13 family of enzymes in a concentration dependent manner (Turner et al., 2004). It may also be the result of a difference in effect across the soluble forms of respective $A\beta_{42}$ oligomers, as specific oligomeric forms are not discernible via ELISA. Additionally, while no enhancement of soluble $A\beta_{x\text{-}42}$ was observed with the vehicle + phosphoramidon treatment (1 or 10 mM), phosphoramidon may need to be administered for a longer period to independently elevate $A\beta_{x\text{-}42}$ levels. Intranasal administration of phosphoramidon was found to increase levels of $A\beta_{42}$, but only after 5 days of administration (Hanson et al., 2011). On a similar line, the neprilysin specific inhibitor thiorphan has also shown to increase levels of $A\beta_{42}$, but also only after continuous infusion for 5 days (Newell et al., 2003).

Evaluations were next performed via Western blot to assess soluble $A\beta_{42}$ oligomers across extracellular, membrane, and intracellular enriched fractions. Soluble Aβ monomers can form oligomeric assemblies ranging from low-molecular weight forms (i.e. dimers and trimers) to higher molecular weight protofibrils. Though the relationship of specific Aβ oligomer species to disease progression remains speculative, support for the general neurotoxicity of soluble $A\beta_{42}$ oligomers has become well recognized. While not all the observed bands assessed have been fully characterized, notable sodium dodecyl sulfate (SDS)-stable bands were shown, consistent with the extraction protocol (Lesne et al., 2006). Such SDS-stable species may present the primary building-blocks for neurotoxic $A\beta_{42}$ oligomers (Larson and Lesne, 2012). The lowest molecular weight $A\beta_{42}$ bands shown corresponded to the trimer (12 kDa) form. It has been proposed that Aβ trimers may constitute the “molecular brick” for non-fibrillar assemblies of Aβ (Larson and Lesne, 2012). Trimers appear to be the most abundant form produced and secreted by primary neurons *in vitro,* with extracellular and intracellular concentrations rising with age in Tg2576 mice (Lesne et al., 2006). Moreover, Aβ trimers have been heavily associated with deficits in long term potentiation (Selkoe, 2008; Townsend et al., 2006). Herein, the $A\beta_{42}$ trimer band showed a decrease within the extracellular and intracellular fractions with NNC 26-9100 treatment, but was not detectable within the membrane fraction. While extracellular alterations in Aβ content have long been affiliated with downstream plaque formation, emerging evidence implicates intracellular accumulation may be more neurotoxic then extracellular Aβ (Casas et al., 2004; Gimenez-Llort et al., 2007).

Additionally, the accumulation of intracellular Aβ has been identified to precede extracellular deposition in both mouse (Oddo et al., 2003) and human (Gouras et al., 2000; Gyure et al., 2001; Mori et al., 2002) studies, implicating an intracellular to extracellular progression of pathology. Significantly, the effect of NNC 26-9100 on the $A\beta_{42}$ trimers was reversed in both the extracellular and intracellular fractions with phosphoramidon co-administration. As neprilysin is understood to catabolize peptides at the levels of the cellular membrane (i.e. ectoenzyme) primarily impacting the membrane and extracellular pool content, the observed intracellular effect would implicate other members of the phosphoramidon-sensitive M13 family. In this regard, ECE-1 (ECE-1b isoform), ECE-2, and NEP2 have intracellular localization, although other yet-undetermined phosphoramidon-sensitive enzymes have been proposed to exist (Nalivaeva et al., 2012; Saido and Leissring, 2012). This understanding would support the idea that NNC 26-9100, through SSTR4 action, impacts multiple members of the M13 family. Nevertheless, to date only neprilysin has shown to degrade oligomeric forms of Aβ (Huang et al., 2006; Kanemitsu et al., 2003), albeit studies of other M13 family enzymes within the context of Aβ are few. If the actions of NNC 26-9100 were specific to neprilysin, then it is also plausible that a cellular compartmental shift in soluble $A\beta_{42}$ could occur. This would result in a default decrease within the intracellular pool as the extracellular levels of soluble $A\beta_{42}$ were reduced. Lastly, the practical implications of isolation/fractionation methodology should be considered, as variables in protocols are often noted with great debate. While any fractionation methodology will have a degree of carry-over into other cellular pools, each fraction would proportionally represent the respective pool identified. Another methodological aspect is the impact of respective isolation/denaturing regents on Aβ oligomers. It has been noted that aggregation/disaggregation may be impacted by particular purification reagents (Masters and Selkoe, 2012). Nevertheless, any such impact would be expected to equally affect both the NNC 26-9100 treated and non treated groups, as the tissue samples were treated identically. In this regard, the overall effect of NNC 26-9100 respective to both the extracellular and intracellular fractions supports its ability to reduce soluble $A\beta_{42}$ trimers.

It has been further hypothesized that Aβ trimers can form larger oligomeric species based on multiples of three (i.e. hexamers, nonamers, and dodecamers) in absence of deposited Aβ (Larson and Lesne, 2012). NNC 26-9100 treatment resulted in a band-split effect of the $A\beta_{42}$ hexamer (extracellular fraction only), which was also reversed by phosphoramidon co-administration. While little is known regarding the hexameric form, a recent evaluation of an antibody (A8) with high affinity and specificity for soluble $A\beta_{42}$ oligomers in the molecular weight range of 16.5-25 kDa was shown to improve learning and memory in SAMP8 mice (8-months of age) (Zhang et al., 2011). This would imply the $A\beta_{42}$ hexamer plays a critical role in learning and memory. Interestingly, while the 56 kDa $A\beta_{42}$ oligomer form was observed in all fractions of the SAMP8 extracted tissue, no changes were shown with NNC 26-9100 or phosphoramidon administration. Previous reports have implicated the extracellular Aβ 56 kDa species (a.k.a. Aβ*56) with impairment of memory independent of plaques or neuronal loss in Tg2576 mice (Lesne et al., 2006). Additionally, levels of Aβ*56 have shown to positively correlate with trimer levels within the respective fractions (Larson and Lesne, 2012; Lesne et al., 2006). Yet, given our experimental design, several qualifiers exist. First, the $A\beta_{42}$ 56 kDa form may simply not be as readily catabolized via enzymatic processes. Given the higher degree of aggregation of the 56 kDa form and single treatment dose of NNC 26-9100 in our paradigm this is quite plausible. Yet, this would also implicate that the $A\beta_{42}$ trimeric and/or hexameric forms are more critical in the learning response, at least in SAMP8 mice. Alternatively, variables in animal model may also be accountable for the observed effect. To date, the studies evaluating Aβ*56 have all been conducted in transgenic mouse models, which substantially overexpress APP. It has been noted that the effects observed in transgenic models may not appropriately reflect the gradual aggregation profile of Aβ seen in late-onset AD (Morley et al., 2012b; Selkoe, 2011), and thus may also

not be appropriately representative of Aβ oligomer alterations or impact. Even amongst transgenic mouse models of AD such as Tg2576 and Tg5469 which express proportional levels of APP show significantly different levels of Aβ, with Aβ trimers not readily shown in the Tg5469 brains (Larson and Lesne, 2012; Ma et al., 2007). To address this issue a group of 12-month old APPswe Tg2576 mice were run against the same optimized dose of NNC 26-9100. A relatively identical enhancement of learning was shown in the Tg2576 mice with NNC 26-9100 treatment. The reduction of the $A\beta_{42}$ trimer was again shown (extracellular and intracellular), as well as the band-split effect of the hexamer form, with NNC 26-9100 treatment. Yet, a decrease in the 56 kDa form within the extracellular fraction was also shown in the Tg2576 mice. This effect may be the result of the Tg2576 mice having the human variant of APP, which could result in subsequent differences in oligomeric aggregation and/or enzymatic affinities. Lastly, Aβ*56 has been identified via numerous Aβ antibodies (Larson and Lesne, 2012), but not the $A\beta_{42}$ specific antibody used herein, as such $A\beta_{40}$ was also evaluated in the Tg2576 fractions. There was greater degree of banding associated of the soluble $A\beta_{40}$ oligomers, which may be attributed to several factors including antibody specificity and a generally higher level of $A\beta_{40}$ in the brain. Nevertheless, a similar reduction trend was shown for the soluble $A\beta_{40}$ and $A\beta_{42}$ oligomers with NNC 26-9100 treatment. While the 56 kDa extracellular band of $A\beta_{40}$ did not show a statistical decrease, the forms at 25 kDa and 12 kDa were reduced with NNC 26-9100 treatment, as were higher molecular weight forms at ~75 kDa and ~63 kDa. Interestingly, there was no substantial effect on intracellular soluble $A\beta_{40}$ oligomers with NNC 26-9100 treatment, which would implicate a differential localization effect between $A\beta_{40}$ and $A\beta_{42}$ oligomers. Also of significance is that the M13 metalloproteinase family is capable of degrading both $A\beta_{40}$ and $A\beta_{42}$ (Nalivaeva et al., 2012; Saido and Leissring, 2012), which further support the hypothesis that NNC 26-9100 is impacting soluble Aβ levels via this family of enzymes.

These data support the hypothesis that the SSTR4 agonist NNC 26-9100 acts via a phosphoramidon-sensitive metalloproteinase-dependent mechanism with regards to observed learning enhancement in SAMP8 mice. These effects correlate to a reduction in soluble $A\beta_{42}$ trimers and a band-split effect of the hexamer. Moreover, the impact of NNC 26-9100 was observed across both a gradual progressive mouse model (SAMP8) and a transgenic APP overexpressing model (Tg2576) of AD. While age-dependent evaluations, in conjunction with assessment of chronic NNC 26-9100 treatment, are required to fully delineate the long term impact of SSTR4 agonist action on learning/memory, enzymatic function, and Aβ alterations, such agonists remain a feasible approach for the treatment of Aβ mediated disease states.

4. Experimental Procedure

4.1 Chemicals

NNC 26-9100, 1-[3-[*N*-(5-Bromopyridin-2-yl)-*N*-(3,4-dichlorobenzyl)amino]propyl]-3-[3-(1*H*-imidazol-4-yl)propyl]thiourea, was synthesized, purified, and confirmed via NMR by Dr. A.M. Crider per previously established protocols (Ankersen et al., 1998; Crider et al., 2004). Unless otherwise stated all other chemicals and reagents were purchased from Sigma-Aldrich (St. Louis, MO, USA).

4.2 Animals

Twelve-month old male SAMP8 or APPswe Tg2576 (model 002789) mice were used for these evaluations. Mice were housed in rooms with a 12 h light/dark cycle (20–22°C) with water and food available *ad libitum*. All experiments were conducted in accordance with the institutional approval of the animal use subcommittee, which subscribes to the NIH Guide

for Care and Use of Laboratory Animals. SAMP8 mice were obtained from the breeding colony at the Veterans Affairs Medical Center - VA Hospital (St. Louis, MO). The Tg2576 mice obtained from Taconic Farms Inc. (New York, USA) and were housed in an identical manner.

4.3 Dosing

NNC 26-9100 treatment was performed via intracerebroventricular (i.c.v.) injection. The i.c.v. dose of NNC 26-9100 (0.2 μg) previously identified to enhance learning in 12-month old SAMP8 mice (Sandoval et al., 2012) was tested against the M13 family inhibitor phosphoramidon (1 or 10 mM) (American Peptide Co, Sunnyvale, CA) via co-administration, and evaluated against respective controls. Previous studies have shown phosphoramidon (i.c.v.) to elevate soluble Aβ levels within 2 h (Eckman et al., 2006).

Briefly, 24 h prior to T-maze testing, the mice were anesthetized with isoflurane, placed in a stereotaxic instrument. The scalp was opened and a unilateral hole was drilled 0.5 mm anterior and 1.0 mm to the right of the bregma. A single i.c.v. (2 μL) injection of NNC 26-9100 (0.2 μg) with or without phosphoramidon (1 or 10 mM), or vehicle control (20% ethanol/saline), was conducted with a 30 g blunt needle connected to a Hamilton syringe, to a depth of 2 mm. Syringe was kept in place via side-arm attachment. Injections were conducted in a gradual manner over ~1 min and syringe was kept in place for 3 s following to assure no back-flow occurred. The hole was filled in with bone-wax and scalp sealed via Vetbond (3M, St. Paul, MN, USA). Subsequent to behavioral evaluations and immediately prior to respective tissue assessments brains were cut along the injection site to assure accuracy.

4.4 T-maze testing

The T-maze foots shock avoidance testing procedures have been previously described and shown to be an effective means to assess learning in SAMP8 mice (Farr et al., 2004; Sandoval et al., 2012). Individual performing test was blind to respective dosing and mice were trained and tested between 07:00 and 15:00 h. The maze consisted of a black plastic start alley with a start box at one end and two goal boxes at the other. A stainless steel rod floor ran throughout the maze. The start box was separated from the start alley by a plastic guillotine door that prevented the mouse from moving down the alley until the training started. A training trial began when a mouse was placed into the start box. The guillotine door was raised and the buzzer was sounded simultaneously; 5 s later, foot shock was applied. The goal box the mouse first entered on the first trial was designated as “incorrect”. Foot shock was continued until the mouse entered the other goal box, which on all subsequent trials was designated “correct” for that specific mouse. At the end of each trial, the mouse was removed from the goal box and returned to its home cage. A new trial began by placing the mouse back in the start box, sounding the buzzer, and raising the guillotine door. Foot shock was applied 5 s later if the mouse did not leave the start box or had not entered the correct goal box.

Training used an intertrial interval of 45 s, and a doorbell type buzzer set at 65 dB as the conditioned stimulus warning of onset of foot shock which was set 0.40 mA (Coulbourn Instruments scrambled grid floor shocker model E13-08). Mice were trained until they made 1 avoidance (acquisition). The acquisition test occurred in single test sessions. Each session lasted from 5 to 15 min. The number of trials to learned avoidance of the incorrect box was determined. The “mean trials to first avoidance” represents acquisition learning. At the end of the acquisition trial, mice were decapitated and the brains snap frozen and stored at −80°C for subsequent analyses.

4.5 Enzyme linked immunosorbent assay

Cortical brain levels of total soluble $A\beta_{x-42}$ were evaluated from tissue following respective behavioral analyses, using ultra-centrifugation and solid-phase extraction methods (Lanz and Schachter, 2006; Zupa-Fernandez et al., 2007), coupled with an enzyme-linked immunosorbent assay (ELISA) analysis (Beta-Mark $A\beta_{x-42}$, Covance) as previously described (Sandoval et al., 2011). Per supplier information the $A\beta_{x-42}$ ELISA has significant reactivity for rodent $A\beta_{1-42}$ and negligible reactivity for $A\beta_{1-40}$. Brain tissue was homogenized using chilled dounce homogenizers using cold 1 mL of 50 mM NaCl, 0.4% diethylamine (DEA), pH=10, containing protease inhibitor (Roche, Indianapolis, IN). Samples were then transferred to ultracentrifuge tubes on ice and kept on ice for 20 minutes prior and during the sonication. Samples were then sonicated at 30% for 30 s and incubated at room temperature for 3 h. Following the 3 h incubation, samples were centrifuged at 355,000 × g for 30 min (4°C) and the supernatant was collected. The supernatant then underwent solid phase extraction using Oasis HLB 3cc columns (Waters, Milford, MA). Oasis columns were activated with 2 mL methanol (MeOH), followed by 2 mL diH_2O. Brain homogenates were loaded in 1 mL increments.

Samples were then washed sequentially with 1 mL volumes of 5% and 30% MeOH, then eluted with 1 mL 2% NH_4OH in 90% MeOH. Eluted samples were collected and vacuum centrifuged at 1400 rpm, 60°C for 90-120 min until reaching dryness. Once samples were dried completely, they were stored at −80°C until assay. Samples were reconstituted and analyzed in duplicate according to ELISA assay directions via luminometer (Lumistar Optima, BMG Labtech, Durham, NC). $A\beta_{x-42}$ levels were calculated from linear regression curve in pg/mL and then set to gram weight of brain tissue and normalized to respective controls.

4.6 Cellular fractionation

Flash frozen cortical tissues were extracted and isolated into soluble extracellular, membrane, and intracellular enriched protein fractions based on the protocol by Lesné et al. (Lesne et al., 2006). Tissues were homogenized (10 strokes with glass Douncer) in 2× vol (w/v) of ice-cold extracellular buffer (50 mM Tris-HCl (pH 7.6), 0.01% NP-40, 150 mM NaCl, 2mM EDTA, 0.1% SDS, 1mM 4-(2-aminoethyl)benzenesulfonyl fluoride hydrochloride (AEBSF), and Complete protease inhibitor (Roche). Samples were then centrifuged at 3,000 rpm at 4°C for 5 min and extracellular-enriched protein fraction was collected (supernatant). Pellets were then gently homogenized in ice-cold intracellular buffer (50 mM Tris-HCl [pH 7.6], 150 mM NaCl, 0.1% Triton X-100, protease inhibitor) (300 μl: cortical & 150 μl: hippocampi) using a micropipettor. Samples were then centrifuged for 13,000 rpm at 4°C for 90 min and cytoplasmic enriched protein fraction was collected (supernatant). Pellets were then homogenized in ice cold membrane buffer (50 mM Tris-HCl [pH 7.4], 150 mM, NaCl, 0.5% Triton X-100, 1 mM EGTA, 3% SDS, 1% deoxycholate, 1 mM AEBSF, and Complete protease inhibitor) (500 μL: cortical tissue) using a micropipettor. Samples were then centrifuged for 13,000 rpm at 4°C for 90 min and membrane enriched protein fraction was collected (supernatant).

Respective samples within each fraction were then immunodepleted by sequential incubation for 1 hr at 4°C on a rotating mixer, with 30 μL of Protein A-Sepharose, followed by 30 μL of Protein G Sepharose, (Fast-Flow®,GE Healthcare Biosciences, Pittsburgh, PA). After each incubation-set samples were filtered from Sepharose via 10 μm pore size filter Spin Cups (Pierce). Following clarification, samples were stored at −80°C for subsequent BCA protein analyses for Western blot examination.

4.7 Western blot analysis

Western blot analyses were performed on the respective enriched cellular fractions, with assessment of $A\beta_{42}$ and $A\beta_{40}$ in respective cortical tissues. The $A\beta_{42}$ antibody (AB5078P, Millipore, Temecula, CA) is reactive for the six amino acid sequence from the C-terminal of $A\beta_{1\text{-}42}$ and does not show appreciable reactivity to $A\beta_{1\text{-}40}$. The $A\beta_{1\text{-}40}$ antibody (SIG 39140, Covance, Dedham, MA, clone: 11A50-B10) is reactive to the C-terminal of Aβ and is specific for the isoform ending at the 40th amino acid. Extracted samples were heated at 95°C for 5 min in 2× SDS and 20× reducing agent (Bio-rad) and loaded into 10% Bis/Tris Criterion XT gels (Bio-Rad). Bands were then separated using an electrophoretic field at 200 V for 35 min in MES running buffer (Bio-Rad). The proteins were then transferred to nitrocellulose membranes with 240 mA at for 30 min (4°C). Following the transfer, the nitrocellulose membranes were boiled for 5 min (sandwiched between filter pads and weighed down in boiling diH_2O) and then blocked in 5% milk-Tris-buffered saline for 4 h or overnight. After all transfers, gels were then evaluated with GelCode Blue Stain (Pierce, Rockford, IL) to confirm appropriate protein loading (Aldridge et al., 2008; Welinder and Ekblad, 2011), as housekeeping protein expression is not optimal for loading confirmation with fractionation procedures. Purified $A\beta_{42}$ peptide was used as a positive control (Sigma, A9810). Blots were developed using the enhanced chemiluminescence method (ECL+, Amersham Life Science Products; Springfield, IL; or SuperSignal West Dura or SuperSignal West Femto, Pierce) and protein bands visualized via ChemiDoc XRS+ (Biorad), and optical densities of expressed bands measured by densitometry via Image Lab software 3.0 (Biorad).

4.8 Statistical analyses

Results were expressed as means ± standard error of the mean (S.E.M). Two-way ANOVA, with Tukey post hoc, performed for multiple-dosing sets (Sigma Stat 3.1). When only two sample groups were evaluated Student's T-test was used. P values less than 0.05 were considered significant.

Acknowledgments

This work was supported by VA Merit Review, and the National Institutes of Health National Institute on Aging (Grant: R21AG029318). A use-patent has been obtained for NNC 26–9100 by Southern Illinois University Edwardsville.

Abbreviations

Aβ	amyloid protein
SSTR	somatostatin receptor subtype
APP	amyloid precursor protein
AD	Alzheimer's disease

References

Aldridge GM, Podrebarac DM, Greenough WT, Weiler IJ. The use of total protein stains as loading controls: an alternative to high-abundance single-protein controls in semi quantitative immunoblotting. J Neurosci Methods. 2008; 172:250–4. [PubMed: 18571732]

Alzheimer's Association. Alzheimer's disease facts and figures. Alzheimers Dement. 2012; 8:131–68. [PubMed: 22404854]

Ankersen M, Crider AM, Liu S, Ho B, Andersen HS, Stidsen CE. Discovery of a Novel Non-Peptide Somatostatin Agonist with SST4 Selectivity. Journal of the American Chemical Society. 1998; 120:1368–1373.

Alzheimer's Association, A. Alzheimer's disease facts and figures. Alzheimers Dement. 2012; 8:131–68. [PubMed: 22404854]

Bruno JF, Xu Y, Song J, Berelowitz M. Molecular cloning and functional expression of a brain specific somatostatin receptor. Proc Natl Acad Sci U S A. 1992; 89:11151–5. [PubMed: 1360663]

Casas C, Sergeant N, Itier JM, Blanchard V, Wirths O, van der Kolk N, Vingtdeux V, van de Steeg E, Ret G, Canton T, Drobecq H, Clark A, Bonici B, Delacourte A, Benavides J, Schmitz C, Tremp G, Bayer TA, Benoit P, Pradier L. Massive CA1/2 neuronal loss with intraneuronal and N-terminal truncated Abeta42 accumulation in a novel Alzheimer transgenic model. Am J Pathol. 2004; 165:1289–300. [PubMed: 15466394]

Crider AM, Liu S, Li T, Mahajan S, Ankersen M, Stidsen CE. Somatostatin receptor subtype 4 (sst4) ligands: Synthesis and evaluation of indol-3-yl and 2-pyridyl-thioureas. Letters in Drug Design & Discovery. 2004; 1:84–87.

Deane R, Bell RD, Sagare A, Zlokovic BV. Clearance of amyloid-beta peptide across the blood-brain barrier: implication for therapies in Alzheimer's disease. CNS Neurol Disord Drug Targets. 2009; 8:16–30. [PubMed: 19275634]

Eckman EA, Reed DK, Eckman CB. Degradation of the Alzheimer's amyloid beta peptide by endothelin-converting enzyme. J Biol Chem. 2001; 276:24540–8. [PubMed: 11337485]

Eckman EA, Adams SK, Troendle FJ, Stodola BA, Kahn MA, Fauq AH, Xiao HD, Bernstein KE, Eckman CB. Regulation of steady-state beta-amyloid levels in the brain by neprilysin and endothelin-converting enzyme but not angiotensin-converting enzyme. J Biol Chem. 2006; 281:30471–8. [PubMed: 16912050]

Epelbaum J, Guillou JL, Gastambide F, Hoyer D, Duron E, Viollet C. Somatostatin, Alzheimer's disease and cognition: An old story coming of age? Prog Neurobiol. 2009

Farr SA, Banks WA, Uezu K, Gaskin FS, Morley JE. DHEAS improves learning and memory in aged SAMP8 mice but not in diabetic mice. Life Sci. 2004; 75:2775–85. [PubMed: 15464829]

Gimenez-Llort L, Blazquez G, Canete T, Johansson B, Oddo S, Tobena A, LaFerla FM, Fernandez-Teruel A. Modeling behavioral and neuronal symptoms of Alzheimer's disease in mice: a role for intraneuronal amyloid. Neurosci Biobehav Rev. 2007; 31:125–47. [PubMed: 17055579]

Gouras GK, Tsai J, Naslund J, Vincent B, Edgar M, Checler F, Greenfield JP, Haroutunian V, Buxbaum JD, Xu H, Greengard P, Relkin NR. Intraneuronal Abeta42 accumulation in human brain. Am J Pathol. 2000; 156:15–20. [PubMed: 10623648]

Gyure KA, Durham R, Stewart WF, Smialek JE, Troncoso JC. Intraneuronal abeta-amyloid precedes development of amyloid plaques in Down syndrome. Arch Pathol Lab Med. 2001; 125:489–92. [PubMed: 11260621]

Hanson LR, Hafez D, Svitak AL, Burns RB, Li X, Frey WH 2nd, Marr RA. Intranasal phosphoramidon increases beta amyloid levels in wild type and NEP/NEP2-deficient mice. J Mol Neurosci. 2011; 43:424–7. [PubMed: 20941644]

Hsiao K, Chapman P, Nilsen S, Eckman C, Harigaya Y, Younkin S, Yang F, Cole G. Correlative memory deficits, Abeta elevation, and amyloid plaques in transgenic mice. Science. 1996; 274:99–102. [PubMed: 8810256]

Huang SM, Mouri A, Kokubo H, Nakajima R, Suemoto T, Higuchi M, Staufenbiel M, Noda Y, Yamaguchi H, Nabeshima T, Saido TC, Iwata N. Neprilysin-sensitive synapse-associated amyloid-beta peptide oligomers impair neuronal plasticity and cognitive function. J Biol Chem. 2006; 281:17941–51. [PubMed: 16636059]

Iwata N, Higuchi M, Saido TC. Metabolism of amyloid-beta peptide and Alzheimer's disease. Pharmacol Ther. 2005; 108:129–48. [PubMed: 16112736]

Jeynes B, Provias J. The case for blood-brain barrier dysfunction in the pathogenesis of Alzheimer's disease. J Neurosci Res. 2011; 89:22–8. [PubMed: 21046564]

Kanemitsu H, Tomiyama T, Mori H. Human neprilysin is capable of degrading amyloid beta peptide not only in the monomeric form but also the pathological oligomeric form. Neurosci Lett. 2003; 350:113–6. [PubMed: 12972166]

Kumar U. Expression of somatostatin receptor subtypes (SSTR1-5) in Alzheimer's disease brain: an immunohistochemical analysis. Neuroscience. 2005; 134:525–38. [PubMed: 15961235]

Lanz TA, Schachter JB. Demonstration of a common artifact in immunosorbent assays of brain extracts: development of a solid-phase extraction protocol to enable measurement of amyloid-beta from wild-type rodent brain. J Neurosci Methods. 2006; 157:71–81. [PubMed: 16678274]

Larson ME, Lesne SE. Soluble Abeta oligomer production and toxicity. J Neurochem. 2012; 120(Suppl 1):125–39. [PubMed: 22121920]

Lesne S, Koh MT, Kotilinek L, Kayed R, Glabe CG, Yang A, Gallagher M, Ashe KH. A specific amyloid-beta protein assembly in the brain impairs memory. Nature. 2006; 440:352–7. [PubMed: 16541076]

Lue LF, Kuo YM, Roher AE, Brachova L, Shen Y, Sue L, Beach T, Kurth JH, Rydel RE, Rogers J. Soluble amyloid beta peptide concentration as a predictor of synaptic change in Alzheimer's disease. Am J Pathol. 1999; 155:853–62. [PubMed: 10487842]

Ma H, Lesne S, Kotilinek L, Steidl-Nichols JV, Sherman M, Younkin L, Younkin S, Forster C, Sergeant N, Delacourte A, Vassar R, Citron M, Kofuji P, Boland LM, Ashe KH. Involvement of beta-site APP cleaving enzyme 1 (BACE1) in amyloid precursor protein mediated enhancement of memory and activity-dependent synaptic plasticity. Proc Natl Acad Sci U S A. 2007; 104:8167–72. [PubMed: 17470798]

Masters CL, Selkoe DJ. Biochemistry of Amyloid beta-Protein and Amyloid Deposits in Alzheimer Disease. Cold Spring Harb Perspect Med. 2012; 2:a006262. [PubMed: 22675658]

Mawuenyega KG, Sigurdson W, Ovod V, Munsell L, Kasten T, Morris JC, Yarasheski KE, Bateman RJ. Decreased clearance of CNS beta-amyloid in Alzheimer's disease. Science. 2010; 330:1774. [PubMed: 21148344]

McLean CA, Cherny RA, Fraser FW, Fuller SJ, Smith MJ, Beyreuther K, Bush AI, Masters CL. Soluble pool of Abeta amyloid as a determinant of severity of neurodegeneration in Alzheimer's disease. Ann Neurol. 1999; 46:860–6. [PubMed: 10589538]

Moller LN, Stidsen CE, Hartmann B, Holst JJ. Somatostatin receptors. Biochim Biophys Acta. 2003; 1616:1–84. [PubMed: 14507421]

Mori C, Spooner ET, Wisniewsk KE, Wisniewski TM, Yamaguch H, Saido TC, Tolan DR, Selkoe DJ, Lemere CA. Intraneuronal Abeta42 accumulation in Down syndrome brain. Amyloid. 2002; 9:88–102. [PubMed: 12440481]

Morley JE, Kumar VB, Bernardo AE, Farr SA, Uezu K, Tumosa N, Flood JF. Beta-amyloid precursor polypeptide in SAMP8 mice affects learning and memory. Peptides. 2000; 21:1761–7. [PubMed: 11150635]

Morley JE, Armbrecht HJ, Farr SA, Kumar VB. The senescence accelerated mouse (SAMP8) as a model for oxidative stress and Alzheimer's disease. Biochim Biophys Acta. 2012a; 1822:650–6. [PubMed: 22142563]

Morley JE, Farr SA, Kumar VB, Armbrecht HJ. The SAMP8 mouse: a model to develop therapeutic interventions for Alzheimer's disease. Curr Pharm Des. 2012b; 18:1123–30. [PubMed: 22288401]

Mucke L, Masliah E, Yu GQ, Mallory M, Rockenstein EM, Tatsuno G, Hu K, Kholodenko D, Johnson Wood K, McConlogue L. High-level neuronal expression of abeta 1-42 in wild-type human amyloid protein precursor transgenic mice: synaptotoxicity without plaque formation. J Neurosci. 2000; 20:4050–8. [PubMed: 10818140]

Nalivaeva NN, Beckett C, Belyaev ND, Turner AJ. Are amyloid-degrading enzymes viable therapeutic targets in Alzheimer's disease? J Neurochem. 2012; 120(Suppl 1):167–85. [PubMed: 22122230]

Newell AJ, Sue LI, Scott S, Rauschkolb PK, Walker DG, Potter PE, Beach TG. Thiorphan-induced neprilysin inhibition raises amyloid beta levels in rabbit cortex and cerebrospinal fluid. Neurosci Lett. 2003; 350:178–80. [PubMed: 14550923]

Oddo S, Caccamo A, Shepherd JD, Murphy MP, Golde TE, Kayed R, Metherate R, Mattson MP, Akbari Y, LaFerla FM. Triple-transgenic model of Alzheimer's disease with plaques and tangles: intracellular Abeta and synaptic dysfunction. Neuron. 2003; 39:409–21. [PubMed: 12895417]

Saido T, Leissring MA. Proteolytic Degradation of Amyloid beta-Protein. Cold Spring Harb Perspect Med. 2012; 2:a006379. [PubMed: 22675659]

Saito T, Iwata N, Tsubuki S, Takaki Y, Takano J, Huang SM, Suemoto T, Higuchi M, Saido TC. Somatostatin regulates brain amyloid beta peptide Abeta42 through modulation of proteolytic degradation. Nat Med. 2005; 11:434–9. [PubMed: 15778722]

Sandoval KE, Farr SA, Banks WA, Niehoff ML, Morley JE, Crider AM, Witt KA. Chronic peripheral administration of somatostatin receptor subtype-4 agonist NNC 26-9100 enhances learning and memory in SAMP8 mice. Eur J Pharmacol. 2011; 654:53–9. [PubMed: 21185826]

Sandoval KE, Farr SA, Banks WA, Crider AM, Morley JE, Witt KA. Somatostatin receptor subtype-4 agonist NNC 26-9100 decreases extracellular and intracellular Abeta(1-42) trimers. Eur J Pharmacol. 2012

Selkoe DJ. Soluble oligomers of the amyloid beta-protein impair synaptic plasticity and behavior. Behav Brain Res. 2008; 192:106–13. [PubMed: 18359102]

Selkoe DJ. Resolving controversies on the path to Alzheimer's therapeutics. Nat Med. 2011; 17:1060–5. [PubMed: 21900936]

Serrano-Pozo A, Frosch MP, Masliah E, Hyman BT. Neuropathological alterations in Alzheimer disease. Cold Spring Harb Perspect Med. 2011; 1:a006189. [PubMed: 22229116]

Shirotani K, Tsubuki S, Iwata N, Takaki Y, Harigaya W, Maruyama K, Kiryu-Seo S, Kiyama H, Iwata H, Tomita T, Iwatsubo T, Saido TC. Neprilysin degrades both amyloid beta peptides 1-40 and 1-42 most rapidly and efficiently among thiorphan- and phosphoramidon sensitive endopeptidases. J Biol Chem. 2001; 276:21895–901. [PubMed: 11278416]

Terry RD, Masliah E, Salmon DP, Butters N, DeTeresa R, Hill R, Hansen LA, Katzman R. Physical basis of cognitive alterations in Alzheimer's disease: synapse loss is the major correlate of cognitive impairment. Ann Neurol. 1991; 30:572–80. [PubMed: 1789684]

Tomobe K, Nomura Y. Neurochemistry, neuropathology, and heredity in SAMP8: a mouse model of senescence. Neurochem Res. 2009; 34:660–9. [PubMed: 19247832]

Townsend M, Shankar GM, Mehta T, Walsh DM, Selkoe DJ. Effects of secreted oligomers of amyloid beta-protein on hippocampal synaptic plasticity: a potent role for trimers. J Physiol. 2006; 572:477–92. [PubMed: 16469784]

Turner AJ, Fisk L, Nalivaeva NN. Targeting amyloid degrading enzymes as therapeutic strategies in neurodegeneration. Ann N Y Acad Sci. 2004; 1035:1–20. [PubMed: 15681797]

Welinder C, Ekblad L. Coomassie staining as loading control in Western blot analysis. J Proteome Res. 2011; 10:1416–9. [PubMed: 21186791]

Zhang Y, He JS, Wang X, Wang J, Bao FX, Pang SY, Yin F, Hu HG, Peng XL, Sun WM, Zheng YP, Hou LL, Hong T. Administration of amyloid-beta42 oligomer-specific monoclonal antibody improved memory performance in SAMP8 mice. J Alzheimers Dis. 2011; 23:551–61. [PubMed: 21297277]

Zupa-Fernandez, A.; Rozzi, AM.; Arnold, HM.; Felsenstein, KM.; Rowley, A.; Treton, G.; Yohrling, G. Society for Neuroscience. Vol. 37th. San Diego: 2007. Optimization of soluble amyloid beta extraction from non transgenic rodents to facilitate the testing of gamma-secretase modulators.

Highlights

- Somatostatin receptor subtype-4 agonist NNC 26-9100 enhanced learning in SAMP8 mice.
- NNC 26-9100 decreased soluble $A\beta_{42}$ oligomer levels in cortical tissue of SAMP8 mice.
- Similar impact on learning and soluble $A\beta_{42}$ oligomer levels shown in Tg2576 mice.
- NNC 26-9100 action was blocked by the metalloproteinase inhibitor phosphoramidon.
- NNC 26-9100 learning and $A\beta_{42}$ oligomer affect shows metalloproteinase-dependence.

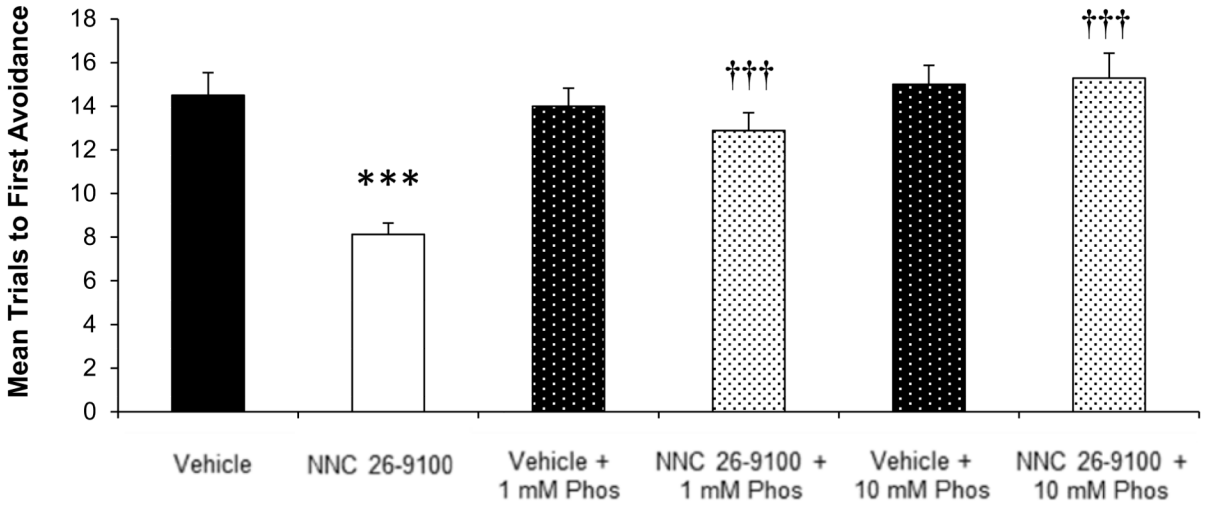

Figure-1.

T-maze acquisition learning in 12-month SAMP8 mice, evaluated 24 h following 2 μL i.c.v. injection of NNC 26-9100 (0.2 μg) or vehicle in the presence of 1 or10 mM phosphoramidon (Phos) (n = 14-16/group). *** $P < 0.001$ compared to vehicle; ††† $P < 0.001$ as compared to NNC-26-9100 alone, two-way ANOVA, values are mean ± S.E.M.

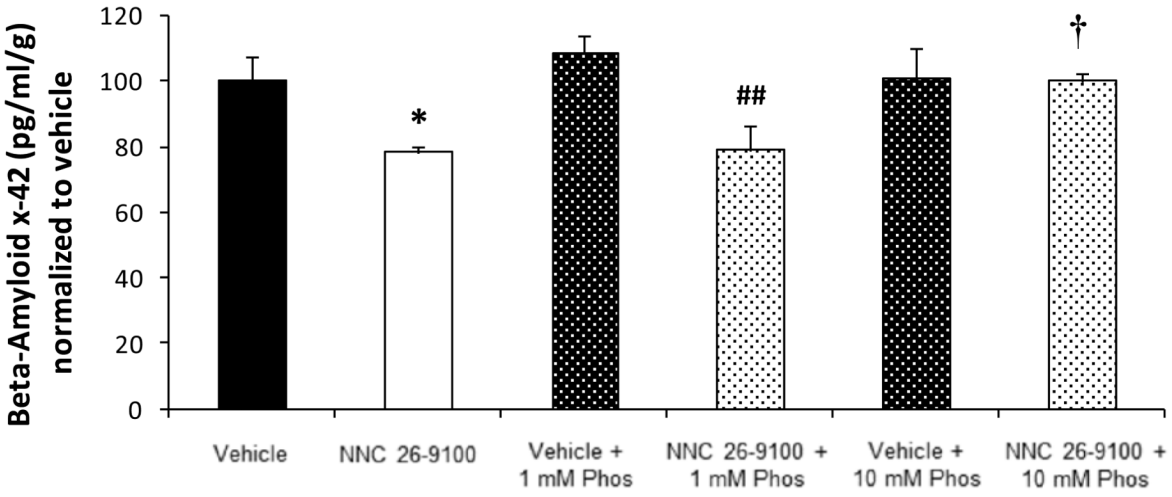

Figure-2.

ELISA analysis of $A\beta_{x\text{-}42}$ performed on cortical tissue extracted from SAMP8 mice following memory retention evaluations of NNC 26-9100 treatment, with and without 1 or10 mM phosphoramidon (Phos). Results calculated as pg/ml/gram of brain tissue and normalized to vehicle (n = 5-6/group). * $P < 0.05$ compared to respective vehicle; ## $P < 0.01$ as compared to vehicle + 1 mM phosphoramidon (Phos); † $P < 0.05$ compared to NNC 26-9100 alone, two-way ANOVA, values are mean ± S.E.M.

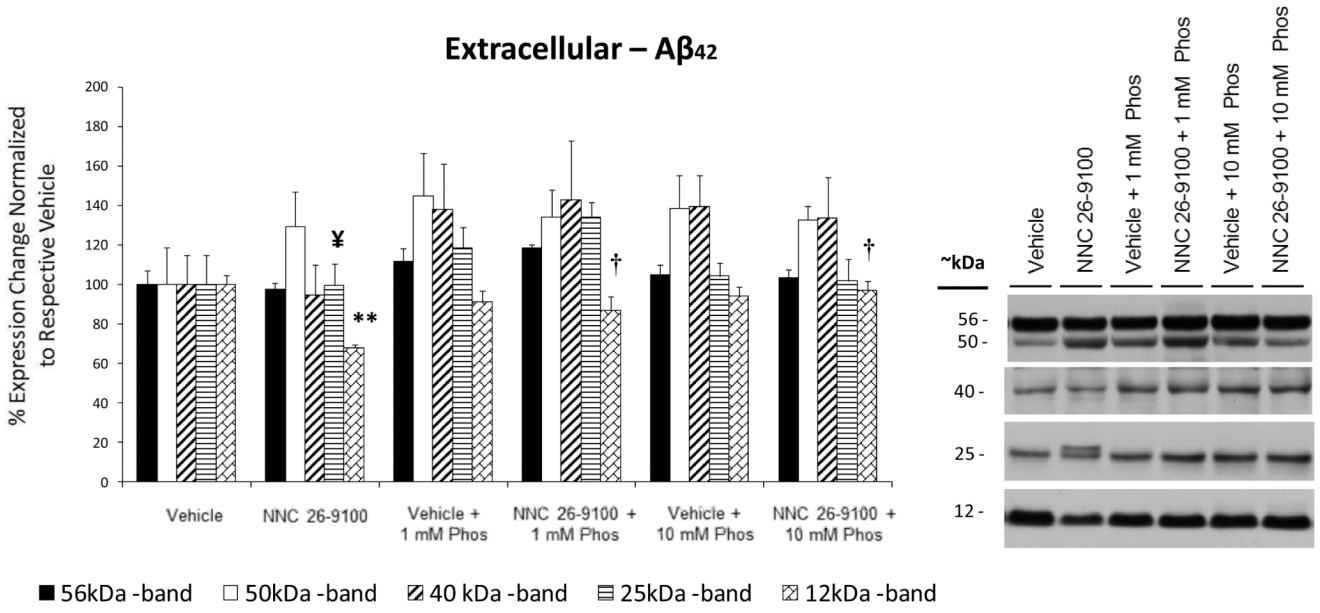

Figure 3.

Western blot of $A\beta_{42}$ from extracellular enriched cellular fractions, respective to NNC 26-9100 and phosphoramidon (Phos) treatment. Soluble oligomeric $A\beta_{42}$ forms identified at 56, 50, 40, 25, and 12 kDa. Protein evaluated with optical densities normalized to respective vehicles ($n = 4$ 5/group). ** $P < 0.01$ compared to respective vehicle; † $P < 0.05$ compared to NNC 26-9100 alone, two way ANOVA, values are mean ± S.E.M. ¥ indicates delineated split of the 25 kDa band with NNC 26-9100 treatment, which was reversed with phosphoramidon treatment (1 or 10 mM). Representative blots shown to right of bar graph.

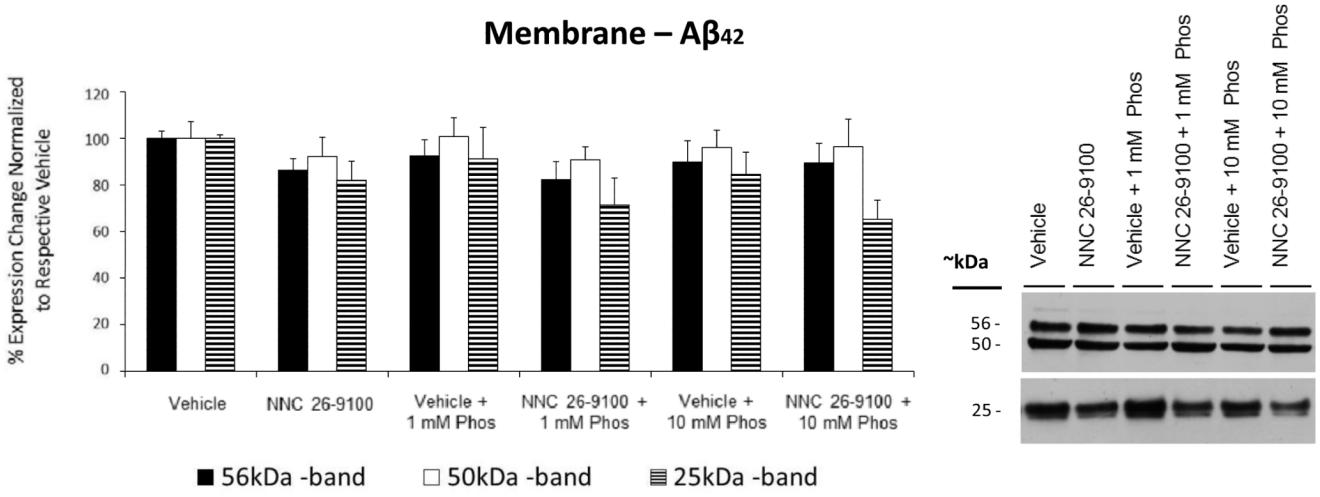

Figure 4.

Western blot of $A\beta_{42}$ from membrane enriched cellular fractions, respective to NNC 26-9100 and phosphoramidon (Phos) treatment. Soluble oligomeric $A\beta_{42}$ forms identified at 56, 50, and 25 kDa. Optical densities normalized to respective vehicles (n = 4 5/group). No statistical significance identified, two way ANOVA, values are mean ± S.E.M. Representative blots shown to right of bar graph.

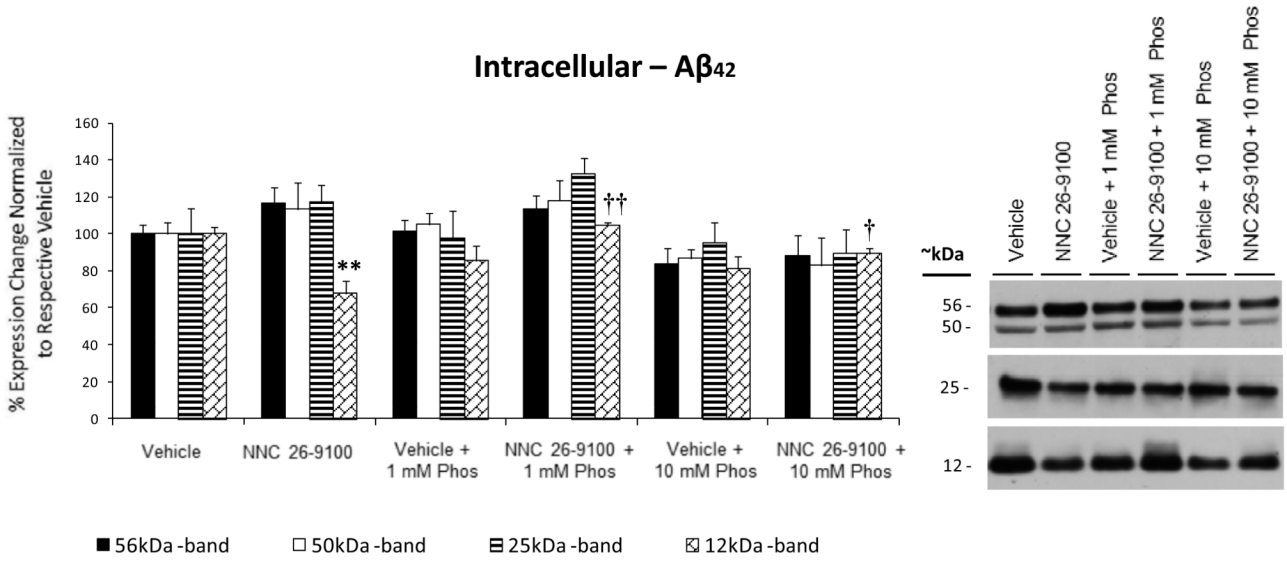

Figure 5.

Western blot of $A\beta_{42}$ from intracellular enriched cellular fractions, respective to NNC 26-9100 and phosphoramidon (Phos) treatment. Soluble oligomeric $A\beta_{42}$ forms identified at 56, 50, 25, and 12 kDa. Optical densities normalized to respective vehicles ($n = 4$ 5/group). ** $P < 0.01$ compared to respective vehicle; † $P < 0.05$, †† $P < 0.01$ as compared to NNC 26-9100 alone, two way ANOVA, values are mean ± S.E.M. Representative blots shown to right of bar graph.

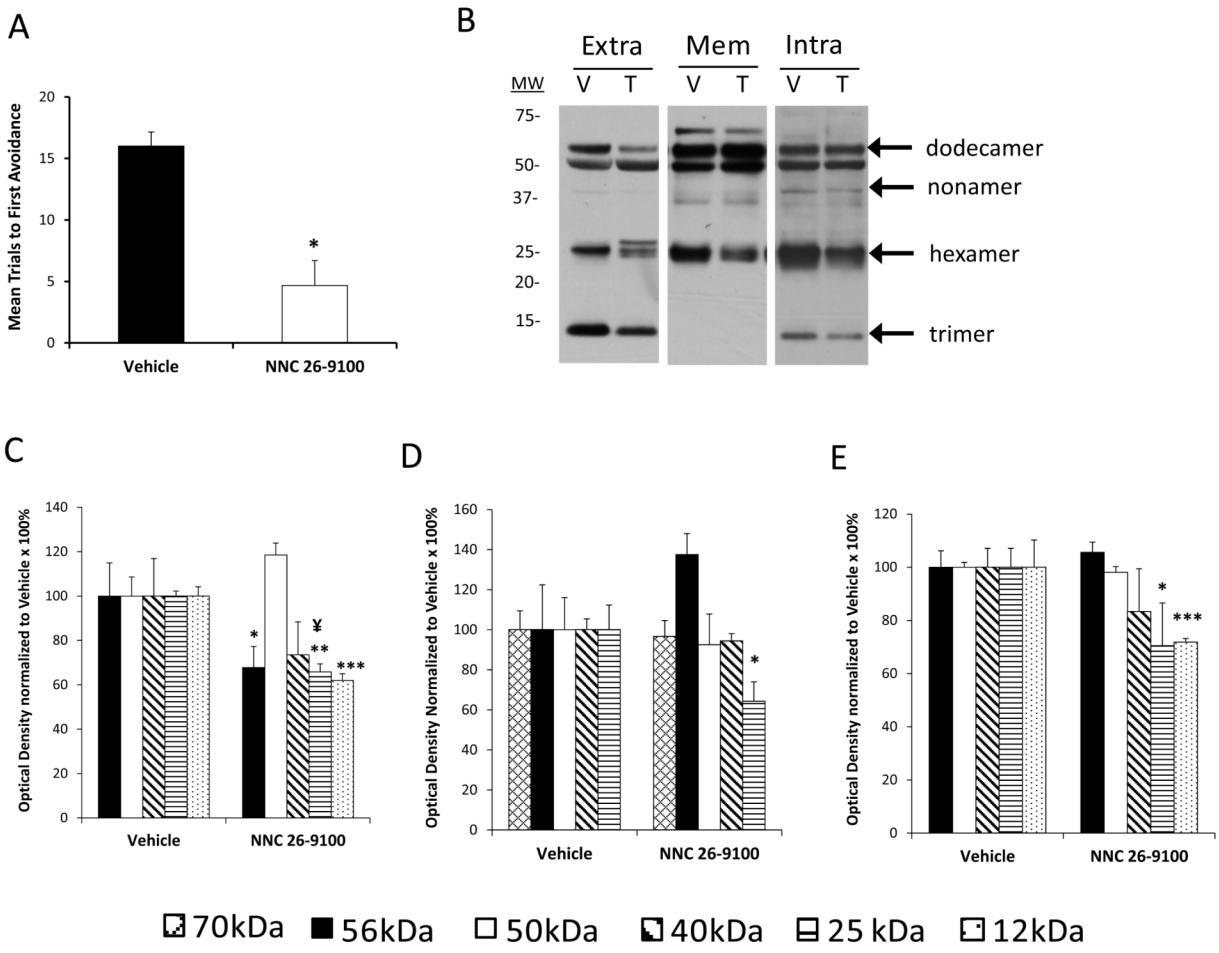

Figure-6.

(A) Acquisition learning of APPswe Tg2576 mice was evaluated using the T-maze task following i.c.v. injection of 0.2 μg NNC 26-9100 (T) or vehicle (V) (n = 3-4/group). (B) Representative Western blot of soluble oligomeric $A\beta_{42}$ forms extracted from extracellular (Extra), membrane (Mem), and intracellular (Intra) fractions (cortical tissue). Bar graphs of $A\beta_{42}$ forms identified within (C) extracellular, (D) membrane, and (E) intracellular fractions. Optical densities normalized to respective vehicles. *$p < 0.05$; ** $p < 0.01$; *** $p < 0.001$ (Student's T-test), values are mean ± S.E.M. ¥ indicates delineated split of the 25 kDa band with NNC 26-9100 treatment.

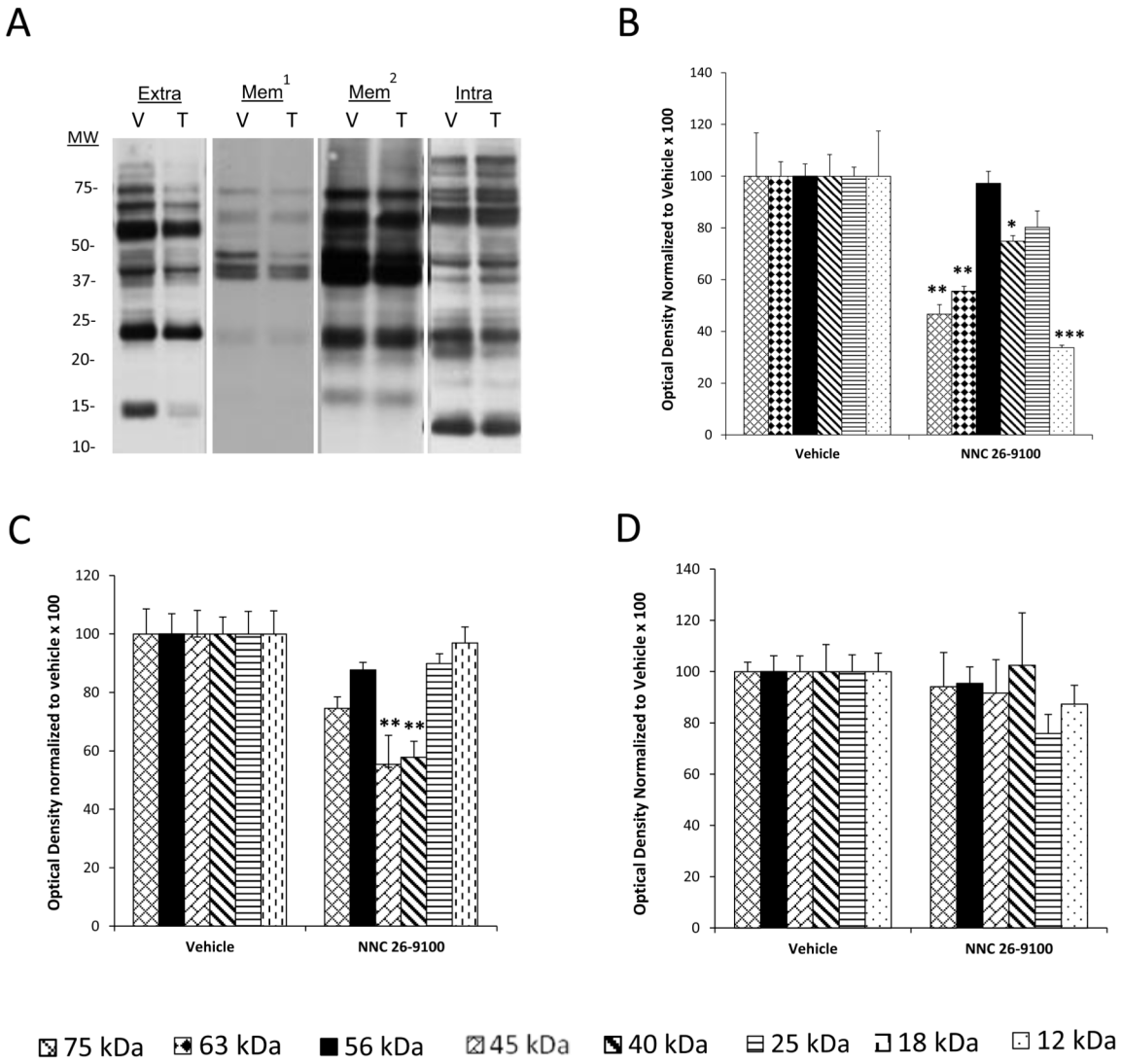

Figure-7.

(A) Representative Western blot of oligomeric $A\beta_{40}$ forms extracted from extracellular (Extra), membrane (Mem^1 - short exposure; Mem^2 - longer exposure), and intracellular (Intra) fractions (cortical tissue) from Tg2576 mice, following i.c.v. injection of 0.2 μg NNC 26-9100 (T) or vehicle (V) (n = 3-4/group). Bar graphs of oligomeric $A\beta_{40}$ forms identified within (B) extracellular, (C) membrane, and (D) intracellular fractions. Optical densities normalized to respective vehicles. *$p < 0.05$; ** $p < 0.01$; *** $p < 0.001$ (Student's T-test), values are mean ± S.E.M.